Biochemical Pharmacology 218 (2023) 115925

Contents lists available at ScienceDirect

Biochemical Pharmacology

journal homepage: www.elsevier.com/locate/biochempharm

# A novel gene signature to diagnose MASLD in metabolically unhealthy obese individuals

Marica Meroni [a], Federica Chiappori [b], Erika Paolini [a,c], Miriam Longo [a], Emilia De Caro [d,e], Ettore Mosca [b], Alice Chiodi [b], Ivan Merelli [b], Sara Badiali [f], Marco Maggioni [g], Alessandra Mezzelani [b], Luca Valenti [h,i], Anna Ludovica Fracanzani [a,h], Paola Dongiovanni [a,*]

[a] Medicine and Metabolic Diseases, Fondazione IRCCS Cà Granda Ospedale Maggiore Policlinico, Milan, Italy
[b] National Research Council - Institute for Biomedical Technologies, (ITB-CNR), 20054 Segrate, Italy
[c] Department of Pharmacological and Biomolecular Sciences, Università degli Studi di Milano, 20133 Milano, Italy
[d] Life and Medical Sciences Institute (LIMES), University of Bonn, Germany
[e] System Medicine, Deutsches Zentrum Für Neurodegenerativen Erkrankugen (DZNE), Bonn, Germany
[f] Department of Surgery, Fondazione IRCCS Cà Granda Ospedale Maggiore Policlinico, Milan, Italy
[g] Department of Pathology, Fondazione IRCCS Cà Granda Ospedale Maggiore Policlinico, Milan, Italy
[h] Department of Pathophysiology and Transplantation, Università degli Studi di Milano, Fondazione IRCCS Cà Granda Ospedale Maggiore Policlinico, Milan, Italy
[i] Precision Medicine Lab, Biological Resource Center, Department of Transfusion Medicine and Hematology, Fondazione IRCCS Ca' Granda Ospedale Maggiore Policlinico, Milan, Italy

ARTICLE INFO

*Keywords:*
Transcriptome
MASLD
VAT
MUHO
Gene signature

ABSTRACT

Visceral adipose tissue (VAT) contributes to metabolic dysfunction-associated steatotic liver disease (MASLD), releasing lipogenic substrates and cytokines which promote inflammation. Metabolic healthy obese individuals (MHO) may shift towards unhealthy ones (MUHO) who develop MASLD, although the mechanisms are still unexplained. Therefore, we aimed to identify dysfunctional pathways and transcriptomic signatures shared by liver and VAT and to outline novel obesity-related biomarkers which feature MASLD in MUHO subjects, at higher risk of progressive liver disease and extrahepatic comorbidities.

We performed RNA-sequencing in 167 hepatic samples and in a subset of 79 matched VAT, stratified in MHO and MUHO. A validation analysis was performed in hepatic samples and primary adipocytes from 12 bariatric patients, by qRT-PCR and western blot.

We identified a transcriptomic signature that discriminate MUHO *vs* MHO, including 498 deregulated genes in liver and 189 in VAT. According to pathway and network analyses, oxidative phosphorylation resulted the only significantly downregulated pathway in both tissues in MUHO subjects. Next, we highlighted 5 genes commonly deregulated in liver and VAT, encompassing *C6*, *IGF1*, *OXA1L*, *NDUFB11* and *KLHL5* and we built a tissue-related score by integrating their expressions. Accordingly to RNAseq data, serum levels of C6 and IGF1, which are the only secreted proteins among those included in the gene signature were downregulated in MUHO *vs* MHO. Finally, the expression pattern of this 5-genes was confirmed in hepatic and VAT samples.

*Abbreviations:* ALT, Alanine Transaminase; AST, Aspartate Transaminase; ANOVA, analysis of variance; AUC, area under the curve; BMI, Body Mass Index; BP, biological processes; CC, cellular components; CI, Confidence Interval; DEGs, differentially expressed genes; ECM, extracellular matrix; EMT, epithelial-mesenchymal transition; ETC, electron transport chain; FDA, Food and Drugs Administration; FDR, false discovery rate; GGT, gamma-glutamil transferase; GO, gene ontology; GoI, Genes of Interest; KEGG, Kyoto Encyclopedia of Genes and Genomes; HCC, hepatocellular carcinoma; HOMA-IR, Homeostatic Model Assessment for Insulin Resistance; IFG, Impaired Fasting Glucose; IGF-1, Insulin-like growth factor 1; IR, insulin resistance, IQR, interquartile range; KLHL5, Kelch Like Family Member 5; LDL, Low Density Lipoproteins; LF, log fold change; MASLD, metabolic dysfunction-associated steatotic liver disease; MF, molecular function; MHO, metabolically healthy obese; MUHO, metabolically unhealthy obese; NAS, NAFLD activity score; MASH, metabolic dysfunction-associated Steatohepatitis; NDUFB11, NADH, ubiquinone oxidoreductase subunit B11; OXA1L, Oxidase (Cytochrome *C*) Assembly 1-like; PC, Principal Component; PCA, Principal Component Analysis; PCR, Principal Component Regression; RNA-seq, RNA-sequencing; ROC, Receiver Operating Characteristic; SD, standard deviation; SVA, Surrogate Variable Analysis; TG, Triglycerides; TGFβ, Transforming Growth Factor Beta; TNFα, Tumor Necrosis Factor Alpha; T2D, Type 2 Diabetes; UPR, unfolded protein response; VLDL, Very Low Density Lipoprotein; VAT, visceral adipose tissue.

* Corresponding author at: Medicine and Metabolic Diseases, Fondazione IRCCS Cà Granda Ospedale Maggiore Policlinico, Milan, Italy.
*E-mail address:* paola.dongiovanni@policlinico.mi.it (P. Dongiovanni).

https://doi.org/10.1016/j.bcp.2023.115925
Received 31 October 2023; Accepted 13 November 2023
Available online 19 November 2023
0006-2952/© 2023 The Authors. Published by Elsevier Inc. This is an open access article under the CC BY-NC license (http://creativecommons.org/licenses/by-nc/4.0/).

We firstly identified the liver and VAT transcriptional phenotype of MUHO and a gene signature associated with the presence of MASLD in these at risk individuals.

## 1. Introduction

Metabolic dysfunction-associated steatotic liver disease (MASLD) is the commonest cause of liver-related morbidity and mortality, affecting more than 30 % of individuals worldwide, mainly as a consequence of the global spreading of obesity, sedentary behaviors, and type 2 diabetes (T2D) [1,2]. MASLD is detectable in more than 70 % of obese subjects and this percentage ramps up to almost 100 % in concurrence with T2D [3]. Obesity is characterized by abnormal visceral adipose tissue (VAT) deposition which contribute to the orchestration of the whole-body metabolic homeostasis, releasing lipogenic substrates, cytokines and hormones and participating to inflammation and oxidative stress [4].

MASLD is depicted by a broad spectrum of hepatic anomalies ranging from simple and reversable steatosis to metabolic dysfunction-associated steatohepatitis (MASH), in which triglyceride overload is entangled with lobular inflammation, ballooning and often with fibrosis. This clinical condition, in predisposed patients with a favorable genetic and acquired make-up, could degenerate into cirrhosis and eventually hepatocellular carcinoma (HCC). To date, a multitude of genetic, epigenetic and environmental MASLD modifiers have been reported [5–7]. Nonetheless, the diagnosis is often delayed due to its unspecific clinical manifestation (i.e., fatigue or slight transaminase enhancement) and its discovery occurs during routine exams. In addition, no Food and Drugs Administration (FDA)-approved drugs exists to treat MASLD and its progressive forms, although several clinical trials are under investigation. Thus, the current therapeutic approach consists in the medication of extra-hepatic comorbidities, whereby managing lifestyle changes, T2D and weight loss. Among the long-term weight-loss adjuvants, bariatric surgery is the most effective to manage obesity and its comorbidities, such as MASLD, T2D, hypertension, dyslipidemia, obstructive sleep apnea and so far [8–11]. Moreover, the gained value of this procedure consists in the possibility to perform intra-operative hepatic biopsies to assess the histological liver damage, thus allowing the clinicians to better manage the post-operative decisions. In our historical cohort of 690 patients who underwent bariatric surgery, more than 84 % already showed signs of MASLD at the time of the intervention, thus emphasizing the role of obesity in the early phases of MASLD and the urgency to identify obesity-related biomarkers. This aspect is even more important if we consider that noninvasive scores for the diagnosis of MASLD and its progressive forms as well as transient elastography not always perform well in patients with morbid and severe obesity [12–14].

In the past years, the liver has been considered the eligible organ to study mechanisms underlying MASLD onset and progression, although an adipocentric perspective is now emerging with the introduction of the paradoxical definition of metabolically healthy obese (MHO) which indicates an adipose tissue compensatory flexibility in maintaining fat storage capacity [7,15]. MHO subjects refer to those with BMI $\geq$ 30 kg/m$^2$ without insulin resistance, dyslipidemia and lower ectopic fat. MHO may gradually shift towards metabolically unhealthy obese (MUHO) who are characterized by glucose intolerance/T2D, increased risk of MASLD, MASH and cardiovascular disease, although they share the same grade of adiposity with MHO.

Herein, we exploited a comprehensive global RNAseq approach to outline transcriptomic changes which occur in MASLD, on a series of hepatic and VAT matched biopsies isolated from severely obese individuals stratified according to MHO and MUHO definitions. Our purpose was to highlight the transcriptional signature shared by liver and VAT and to outline novel obesity-related biomarkers to discriminate

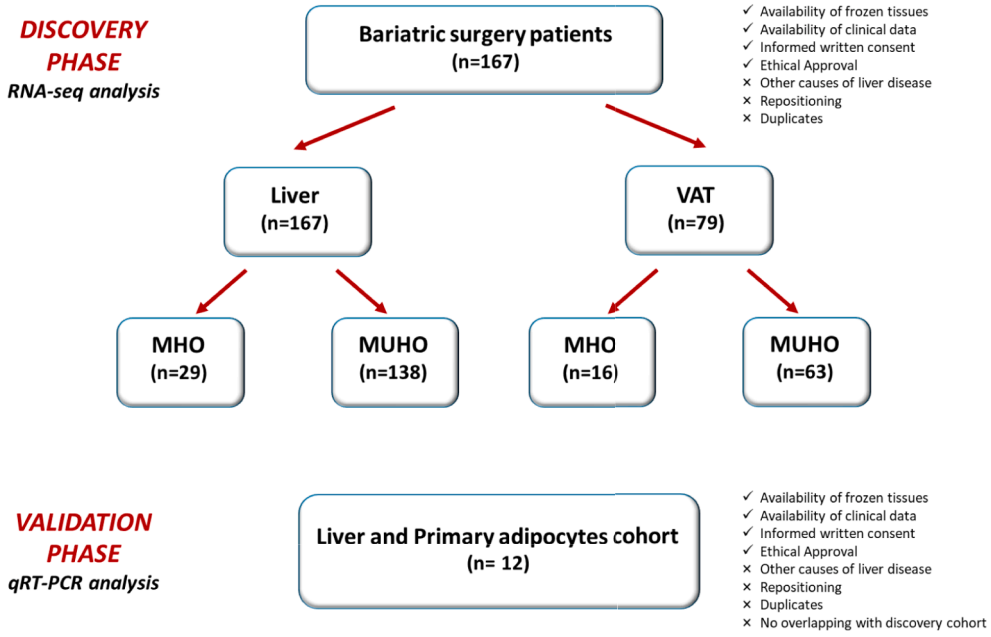


**Fig. 1.** Experimental study design. A total of 167 obese individuals who underwent bariatric surgery were included in the discovery phase of this study (Bariatric Surgery cohort). RNA-seq analysis was performed in hepatic samples from the entire cohort (n = 167) and in 79 matched visceral adipose tissue (VAT) samples from a subgroup of patients. According to the Wildman definition (41), we stratified patients in metabolically healthy (MHO) and unhealthy (MUHO) obese individuals, characterized by the presence of dyslipidemia, insulin resistance, elevated transaminase levels and MASLD. For hepatic trascriptome n = 29 MHO with normal liver and 138 MUHO with MASLD were enrolled, whereas matched VAT specimens from n = 16 MHO and 63 MUHO with MASLD were available. For the validation phase, common biomarkers identified have been assessed by qRT-PCR in livers and primary adipocytes isolated from 12 obese indivuals with the same features of those belonging to the Bariatric Surgery cohort.

**Table 1**
Demographic, anthropometric and clinical features of 167 severely obese patients (Bariatric surgery cohort).

| Liver | Bariatric surgery cohort (overall) (n = 167) | MHO (n = 29) | MUHO (n = 138) | *P*-value |
|---|---|---|---|---|
| Sex, M/F | 28/139 | 2/27 | 36/112 | 0.13* |
| Age, years | 43 ± 10 | 42 ± 7.6 | 43 ± 11 | 0.58 |
| BMI, kg/m2 | 41.3 ± 7.4 | 38 ± 8.7 | 42 ± 6.9 | 0.006 |
| IFG/T2D (0/1) | 150/17 | 29/0 | 121/17 | 0.21* |
| Glucose, mg/dL | 98 ± 27 | 88 ± 10 | 100 ± 28 | 0.04 |
| Insulin, U/L | 21 {12–29} | 9 {7–12} | 22 {13–32} | 0.006 |
| HOMA-IR | 5.3 ± 3.6 | 2.1 ± 0.8 | 5.9 ± 3.6 | 0.002 |
| HbA1c, mmol/mol | 40 ± 7 | 35 ± 2.2 | 41 ± 7.5 | 0.04 |
| Total chol, mmol/L | 5.3 ± 1.2 | 5.2 ± 1.4 | 5.3 ± 1.1 | 0.76 |
| LDL chol, mmol/L | 3.3 ± 0.9 | 3.5 ± 0.8 | 3.3 ± 0.9 | 0.41 |
| HDL chol, mmoL/L | 1.4 ± 0.35 | 1.6 ± 0.3 | 1.4 ± 0.3 | 0.007 |
| Triglycerides (TG), mmoL/L | 1.45 ± 0.7 | 1.1 ± 0.5 | 1.5 ± 0.7 | 0.02 |
| TG/HDL ratio | 1.1 ± 0.7 | 0.7 ± 0.3 | 1.2 ± 0.8 | 0.008 |
| Dyslipidemia (0/1) | 136/31 | 29/0 | 107/31 | 0.07 |
| ALT, IU/l | 16 {20–30} | 11 {16–22} | 21 {17–33} | <0.0001 |
| AST, IU/l | 15 {18–24} | 14 {16–20} | 19 {15–25} | 0.01 |
| GGT, IU/l | 15 {24–43} | 8 {16–28} | 29 {19–49} | 0.06 |
| Hypertension (0/1) | 111/56 | 26/3 | 85/53 | 0.08 |
| Steatosis ≥ 2, yes (%) | 82 (49) | 0 | 82 (60) | <0.0001* |
| Lobular inflammation ≥ 1, yes (%) | 94 (56) | 0 | 94 (68) | <0.0001* |
| Ballooning ≥ 1, yes (%) | 24 (14) | 0 | 24 (17) | 0.001* |
| Fibrosis ≥ 2, yes (%) | 13 (8) | 0 | 13 (9) | 0.02* |
| NAS > 5, yes (%) | 22 (13) | 0 | 22 (16) | 0.002* |
| HSI | 50.6 ± 7.5 | 49.0 ± 8.2 | 50.9 ± 7.3 | 0.21 |
| BAAT | 1.6 ± 0.7 | 1.25 ± 0.6 | 1.65 ± 0.8 | 0.03 |
| FIB-4 | 0.8 ± 0.5 | 0.74 ± 0.4 | 0.74 ± 0.5 | 0.92 |

Values are reported as mean ± SD or median {IQR}as appropriate. BMI: body mass index; IFG: impaired fasting; T2D: type 2 diabetes mellitus; NAS: NAFLD activity score. *p-value at chi-squared test.

MUHO, at higher risk to develop MASLD and its progressive forms as well as extrahepatic comorbidities.

## 2. Materials and methods

### 2.1. Study design and patient selection

A total of 167 obese subjects (Bariatric surgery cohort) who underwent percutaneous liver and adipose tissue biopsies during bariatric surgery at Fondazione IRCCS Cà Granda, Ospedale Policlinico, Milan were enrolled [16]. Bulk RNA-seq analysis was performed in hepatic samples from the overall cohort (n = 167) and in matched adipose tissues from a subgroup of patients (n = 79). According to the Wildman definition, the Bariatric surgery cohort was subdivided in 29 metabolic healthy (MHO) and 138 metabolic unhealthy (MUHO) (Fig. 1, Table 1). At histological evaluation, only MUHO patients had MASLD (Table 1).

Individuals with excessive alcohol intake (men, >30 g/day; women, >20 g/day), viral and autoimmune hepatitis, hereditary hemochromatosis and alpha1-antitrypsin deficiency or other causes of liver diseases were excluded [17].

Informed written consent was obtained from each patient and the study protocol was approved by the Ethical Committees of Fondazione IRCCS Cà Granda, Milan and it conformed to the 1975 Declaration of Helsinki (CE n. 164_2019). Study design and clinical features of enrolled patients are represented in Fig. 1 and Table 1.

### 2.2. Biochemical evaluations

Body mass index (BMI) was calculated by dividing the body weight for the squared height. T2D was diagnosed when impaired fasting glucose tolerance was present and fasting glucose > 110 mg/dL. Alanine aminotransferase (ALT), aspartate aminotransferase (AST), gamma-glutamil transferase (GGT), triglycerides, total cholesterol, HDL and LDL were measured by standard laboratory methods [18]. Dyslipidemia was defined according to the American heart Association's classification as total cholesterol > 5.2 mmol/L, LDL > 3.4 mmol/L, triglycerides (TG) ≥ 1.70 mmol/L and HDL < 1.0 mmol/L or a combination thereof [19].

The presence of hypertension was defined when systolic blood pressure was over 140 mmHg or diastolic blood pressure over 90 mmHg more than twice or in subjects treated with anti-hypertensive medication whereas pre-hypertension was defined when systolic blood pressure was ≥ 120 to 139 mmHg or diastolic blood pressure ≥ 80 to 89 mmHg.

### 2.3. Histological and liver damage evaluation

Steatosis was graded according to the percentage of affected hepatocytes as 0: 0–4 %, 1: 5–32 %, 2: 33–65 %, 3: 66–100 %. Disease activity was assessed according to the MASLD Activity Score (NAS) with systematic evaluation of steatosis, hepatocellular ballooning and necroinflammation; fibrosis was staged according to the recommendations of the MASLD clinical research network [20]. Liver biopsies scoring was performed by two expert pathologists unaware of patients' status and genotype [21]. The concordance between pathologists was good for fibrosis and steatosis with a coefficient of interobserver agreement of 0.89 and 0.76, respectively. MASH was defined as the concomitant presence of steatosis, lobular inflammation and ballooning.

### 2.4. Transcriptomic and bioinformatic analysis

Total RNA was isolated using RNeasy mini-kit (Qiagen, Hulsterweg, Germany). RNA quantification and quality control were determined by NanoDrop ND-1000 spectrophotometer and Agilent 2100 Bioanalyzer (ThermoFisher Scientific, Carlsbad, USA), respectively. Samples with RNA Integrity Number (RIN) ≥ 7 were used for library preparation. RNA sequencing was performed as previously described [22].

To remove possible batch effect and unwanted sources of variation we applied a Surrogate Variable Analysis (SVA; v3.35.2) [23] using measured demographic and clinical features (Age, Sex, BMI, ALT, AST, T2D) and batch conditions as known source of variations. Thus, the surrogate variables obtained as SVA-output were used as covariates to adjust for latent sources of noise in subsequent differentially expressed genes (DEGs) analysis. The differential expression analysis was performed through R/Bioconductor package DESeq2 (v1.28.1) [24]. We defined DEGs those with a p-value corrected by Benjamini-Hochberg false discovery rate (FDR) lower than 0.05 and fold change (LF) > |0|.

To identify differentially expressed pathways, Generally Applicable Gene-set Enrichment (GAGE v2.38.3) was performed on protein coding genes [25]. The GAGE analysis was set against Kyoto Encyclopedia of Genes and Genomes (KEGG) [26], Molecular Signatures Database, c5-ontology gene sets (MSigDB-c5) (hereafter HALLMARK) [27] and Gene Ontology (GO)-terms [28] as reference databases, separately. GO analysis was also performed to explore the functional role of protein coding genes in terms of biological processes (BP), molecular function (MF) and cellular component (CC). The resulting GO-terms of each GO-category (BP, MF and CC) were clustered according to their similarity employing the binary cut method [29] integrated in the R/Bioconductor package "simplifyEnrichment" thus minimizing the redundancy of GO-terms [29].

We performed Gene Set Variation Analysis (GSVA) to estimate variation of GoI over the presence of MASLD in an unsupervised manner. GSVA scores were calculated by using the deviation method (DE) set for genes signature that might have a different regulation ("up" and "down") across the groups [30,31], then a *t*-test was applied to calculate the mean variation of those scores between groups.

To assess the diagnostic performance of biomarkers shared by hepatic and adipose tissue in predicting MASLD, we constructed Receiver Operating Characteristic (ROC) curves and calculated the Area Under the Curves (AUROC) by exploiting the R package CombiROC [32]. We tested biomarkers alone or combined together through a logistic regression relying on a generalized linear model considering a binomial distribution. Briefly, the software starts by performing a combinatorial analysis which takes as input the data corresponding to the two classes of samples to be compared in a pairwise manner and computes combinations of biomarkers.

### 2.5. Cell-Cell communication inference

Hepatic and VAT upregulated and down-regulated DEGs with a p-adj $< 0.05$ obtained from the comparison MUHO *vs* MHO were screened to quantify the presence of Ligand-Receptor interactions between the two tissues. We exploited the comprehensive database OmniPath [33], which includes more than 100 intracellular and intercellular resources to infer cell–cell communication, protein localization and secretion from transcriptomics data. OmniPath's intra- and intercellular components are both available via the OmnipathR package (v3.0.4) (https://github.com/saezlab/OmnipathR). Each DEG was associated with a score, calculated as the product between the -log10 of differential expression p-value and log2 of the fold change. The strength of the interaction was quantified as the product of the corresponding scores. Subcellular localization and information about secretion were collected from the Human Protein Atlas [34].

### 2.6. Network analysis: Parameter optimization and gene network enrichment in DEGs

The biological network analysis tool "dmfind" [35] (https://github.com/emosca-cnr/dmfind002) was used to analyze the protein–protein interactions (PPI) among DEGs. Briefly, dmfind uses network diffusion [36] to prioritize DEGs by means of the permutation-adjusted "network smoothing index" (*Sp*), a gene-level score that reflects both the significance of a DEG and its network proximity to other DEGs in a genome-wide interactome. The interactome was defined using PPIs from STRING (v11) with confidence score higher than 0.7 [37], excluding text mining as evidence type. To define the initial gene-level scores for the diffusion process, the fold change (FC) and *p*-value resulting from differential expression analysis were combined into $x_0 = -\log_{10}(p) \bullet |\log_2(FC)|$, only for genes with $p < 0.05$ and $|\log_2(FC)| > \log_2(1.5)$, while $x_0$ was set to 0 for all other genes to reduce noise. The network diffusion weighting parameter α was set to 0.7, as in previous works [35], while the parameter $\varepsilon$ – appearing in the definition of *Sp* – was set to the value that maximizes the presence of connected genes with high $x_0$ values among the top ranking genes by decreasing *Sp* [38].

We selected the values of the parameter $\varepsilon$ in order to maximize the presence of connected genes with high initial scores among the genes ranked by decreasing permutation-adjusted network smoothing index $Sp(\varepsilon)$, analogously to what was described in Di Nanni *et al.* [36].

The optimal values of $\varepsilon$ used in the analyses in this study are the followings:

| | NvC Liver | NvC Adipose |
|---|---|---|
| $\varepsilon$ | 1 | 1 |

Lastly, the "top networks" were defined considering 300 top ranking genes (ranked by *Sp*) that ensured the statistical enrichment in DEGs in all the comparisons by using the Gene Set Enrichment Analysis (GSEA) procedure. In particular, we considered the ranked list of all genes by decreasing initial score $x_0$ and tested the enrichment of the gene sets defined by the top *r* ranking genes by decreasing *Sp* that form connected networks, that is, excluding those genes that are not linked to any of the other *r*-1 genes. A high enrichment indicates that the connected network contains a relatively high number of DEGs. A total of 100 permutations was used for statistical assessment. Community detection and centrality analyses were performed using the R package igraph (https://igraph.org). The enrichment of network communities, identified as densely connected sets of genes that reflect specific biological functions [35], in HALLMARK gene sets from MSigDB [27] was assessed by hypergeometric test Nominal p-values were corrected using the Benjamini-Hochberg procedure.

### 2.7. Evaluation of circulating C6 and IGF-1

Circulating levels of C6 and IGF-1 were assessed in duplicate by using Human Complement C6 ELISA kit and Human IGF-1 ELISA kit (Abcam, Cambridge, UK) on serum samples collected at the time of liver biopsy after overnight fasting and stored at − 80 °C. The lowest limit of sensitivity was 71 pg/mL and 11.97 pg/mL for C6 and IGF-1, respectively, according to manufacturer instructions.

### 2.8. Isolation and differentiation of mesenchymal stem cells from human adipose tissue

VAT specimens were obtained from 12 subjects, who underwent bariatric surgery at Fondazione IRCCS Cà Granda. Adipose tissue was digested with type I collagenase 1 mg/ml (Sigma-Aldrich) at 37 °C for 30–60 min. The suspension was centrifuged at 500 g for 1 min to separate the pelleted stromal vascular component from the floating one contaninig the human mesenchymal stem cells (hMSC). The latter were then resuspended in Dulbecco's modified Eagle's medium (DMEM) supplemented with HEPES (15 mM), glucose (25 mM), bovine serum albumin (1 %), 50 nM adenosine, antibiotics, and 1 % fetal bovine serum.

hMSC were differentiated into adipocytes using an adipogenic cocktail in normoxic conditions for 5 days. The standard adipogenic cocktail consisted of 10 % FBS–high-glucose DMEM plus (Gibco), 1.5 μM insulin (Novo Nordisk), 1 μM dexamethasone (Sigma), 500 μM 3-isobutyl-1-methylxanthine (Sigma), and 2 μM rosiglitazone (Sigma) [39].

### 2.9. Gene and protein expression analysis

RNA was extracted from 50 mg of tissue and from cell cultures using Trizol reagent (Life Technologies-ThermoFisher Scientific, Carlsbad, U.S.A). 1 μg of total RNA was *retro*-transcribed with VILO random hexamers synthesis system. Quantitative real time PCR (qRT-PCR) was performed by QuantStudio3 Real Time, Fast SYBR Green chemistry (Fast SYBR Green Master Mix; Life Technologies) for gene expression. All reactions were delivered in triplicate. Data were normalized to the β-actin gene expression as housekeeping and results were expressed as arbitrary units (AU) or fold increase as indicated in bar graphs.

Total protein lysates were extracted from 50 mg of tissues or from cell cultures using RIPA buffer containing protease and phosphatase inhibitors. To optimize protein extraction from VAT we applied a Removal of Excess Lipids (RELi) method to reduce lipid contamination [40].

Equal amounts of proteins (50 μg) were separated by SDS-PAGE, transferred electrophoretically to nitrocellulose membrane (BioRad, Hercules, CA) and incubated with specific antibodies directed against OXA1L (Mouse Polyclonal Anti-OXA1L 1:1000, ab88975 Abcam), NDUFB11 (Rabbit Recombinant Monoclonal Anti-NDUFB11 1:1000, ab183716 Abcam), KLHL5 (Rabbit Polyclonal Anti-KLHL5 1:1000,

**Table 2**
Demographic, anthropometric and clinical features of 79 severely obese patients of whom adipose tissue RNAseq data was available.

| Adipose tissue | Bariatric surgery cohort (subgroup) (n = 79) | MHO (n = 16) | MUHO (n = 63) | *P*-value |
|---|---|---|---|---|
| Sex, M/F | 16/63 | 1/15 | 15/48 | 0.15* |
| Age, years | 44.1 ± 9.6 | 44.2 ± 8.2 | 44 ± 9.9 | 0.34 |
| BMI, kg/m2 | 41.6 ± 7.1 | 39.9 ± 10.2 | 42 ± 6.2 | 0.003 |
| IFG/T2D (0/1) | 69/10 | 16/0 | 53/10 | 0.40* |
| Glucose, mg/dL | 97.5 ± 16 | 88 ± 9 | 100 ± 16 | 0.04 |
| Insulin, U/L | 18 {12–30} | 9 {8–11} | 21 {13–33} | 0.008 |
| HOMA-IR | 5.4 ± 3.8 | 2 ± 0.4 | 6.2 ± 3.8 | 0.01 |
| HbA1c, mmol/mol | 40.5 ± 7 | 35 ± 3 | 41 ± 7.5 | 0.04 |
| Total chol, mmol/L | 5.2 ± 0.9 | 5.5 ± 0.95 | 5.8 ± 0.9 | 0.15 |
| LDL chol, mmol/L | 3.2 ± 0.9 | 3.4 ± 0.8 | 3.1 ± 0.9 | 0.35 |
| HDL chol, mmoL/L | 1.5 ± 0.35 | 1.7 ± 0.4 | 1.4 ± 0.3 | 0.005 |
| Triglycerides, mmoL/L | 1.4 ± 0.7 | 0.95 ± 0.4 | 1.5 ± 0.7 | 0.009 |
| Dyslipidemia (0/1) | 66/13 | 16/0 | 50/13 | 0.01 |
| ALT, IU/l | 21 {16–29} | 19 {13–22} | 21 {16–31} | 0.01 |
| AST, IU/l | 19 {16–25} | 16 {13–22} | 19 {16–25} | 0.16 |
| GGT, IU/l | 25 {20–43} | 21 {14–30} | 25 {21–45} | 0.07 |
| Hypertension (0/1) | 51/27 | 13/3 | 39/24 | 0.36 |
| Steatosis ≥ 2, yes (%) | 42 (53) | 0 | 42 (67) | <0.0001* |
| Lobular inflammation ≥ 1, yes (%) | 50 (63) | 0 | 50 (79) | <0.0001* |
| Ballooning ≥ 1, yes (%) | 15 (19) | 0 | 15 (24) | <0.0001* |
| Fibrosis ≥ 2, yes (%) | 7 (9) | 0 | 7 (11) | <0.0001* |
| NAS > 5, yes (%) | 13 (16) | 0 | 13 (21) | <0.0001* |
| HSI | 50.9 ± 7.2 | 50.6 ± 9.7 | 50.9 ± 6.6 | 0.87 |
| BAAT | 1.6 ± 0.7 | 1.27 ± 0.5 | 1.72 ± 0.7 | 0.05 |
| FIB-4 | 0.8 ± 0.3 | 0.81 ± 0.4 | 0.73 ± 0.3 | 0.40 |

Values are reported as mean ± SD or median {IQR}as appropriate. BMI: body mass index; IFG: impaired fasting; T2D: type 2 diabetes mellitus; NAS: NAFLD activity score. *p-value at chi-squared test.

HPA013958 Merck). Equal amount of samples were pooled prior electrophoretic separation and all reactions were performed in duplicate and ran together in the same gel. Protein levels were quantify by ImageJ software (version 1.52 a) and normalized on vinculin (Rabbit polyclonal Anti-Vinculin 1:5000, ab73412 Abcam), as housekeeping gene.

### 2.10. Statistics

For descriptive statistics, continuous variables were shown as mean and standard deviation (SD) whereas categoric variables were presented as number and proportion. Highly skewed biological variables were reported as median and interquartile range (IQR) and were log-transformed before analyses. Kruskal-Wallis or $\chi 2$ tests were applied to test differences between non categoric and categoric variables, respectively. In the transcriptome analysis, p-values were corrected for multiplicity by Benjamini-Hochberg method, and adjusted p-values $< 0.05$ were considered statistically significant. Statistical analyses were carried out using R software v.4.0.4 (https://www.r-project.org) and JMP-Pro 16.1 (SAS, Cary, NC).

**Table 3**
List of the main hepatic up- and dowregulated coding and non-coding genes in the comparison MUHO *vs* MHO.

| Upregulated | | | Down-regulated | | |
|---|---|---|---|---|---|
| **Genes** | **p-value** | **p-adj** | **Genes** | **p-value** | **p-adj** |
| ENO3 | 2.2E-08 | 5.3E-05 | APOF | 4.5E-09 | 3.0E-05 |
| TSPAN3 | 1.8E-08 | 5.3E-05 | KARS1 | 1.5E-08 | 5.3E-05 |
| TNK2 | 7.4E-08 | 0.0001 | SHBG | 1.4E-07 | 0.0001 |
| ZBTB33 | 7.8E-08 | 0.0001 | ALDH6A1 | 3.2E-07 | 0.0003 |
| FNDC5 | 2.7E-07 | 0.0003 | GPC3 | 9.9E-06 | 0.003 |
| SMAD5 | 1.4E-06 | 0.0008 | SOD1 | 1.0E-05 | 0.003 |
| PLXNA4 | 3.8E-06 | 0.002 | IGF1 | 1.3E-05 | 0.003 |
| OPTN | 5.9E-06 | 0.002 | NDUFB1 | 1.7E-05 | 0.004 |
| CIDEC | 9.4E-05 | 0.010 | ITLN1 | 4.8E-05 | 0.007 |
| LPL | 0.0002 | 0.01 | FGL1 | 6.9E-05 | 0.009 |
| **Non-coding** | **p-value** | **p-adj** | **Non-coding** | **p-value** | **p-adj** |
| AJ009632.2 | 6.2E-09 | 3.00E-05 | DIO3OS | 2.6E-07 | 0.0002 |
| GLTPD2 | 1.4E-06 | 0.0008 | LINC01702 | 9.9E-06 | 0.003 |
| AC022506.2 | 6.3E-06 | 0.002 | MIR193BHG | 3.7E-05 | 0.006 |

## 3. Results

### 3.1. Clinical and histopathologic features of patients in the bariatric surgery cohort

The clinical characteristics of patients enrolled in the study (n = 167) and of those belonging to the subgroup (n = 79) whose matched adipose tissues were available are summarized in Table 1 and 2**,** respectively. The mean age of participants was 43 ± 10 and women composed the majority of the cohort (83 %; n = 139). The mean body mass index (BMI) was 41.3 ± 7.4 and metabolic comorbidities included type 2 diabetes (T2D, 10 %; n = 17), hypertension (34 %; n = 56) and dyslipidemia (19 %; n = 31). According to Wildman definition patients were clustered in two categories: metabolic healthy (17 %; n = 29, MHO), and metabolic unhealthy (83 %; n = 138; MUHO). Specifically, MHO had not insulin resistance and T2D with HOMA-IR ≤ 5.1, a TG/HDL ≤ 1.32, absence of dyslipidemia. Three out 29 of MHO patients presented pre-hypertension. At histological classification, MHO patients didn't show liver disease (Table 1).

Conversely, MUHO patients presented glucose intolerance/T2D (HOMA-IR ⩾5.1; p = 0.002), dyslipidemia with higher TG (p = 0.02), hypertension (p = 0.08) and higher transaminase levels (p < 0.01). In addition, all MUHO patients had histological diagnosis of MASLD. Among them 60 % had steatosis ⩾2, 68 % lobular inflammation ⩾1, 17 % ballooning ⩾1, 9 % fibrosis ⩾2, 54 % MASH and 36 % MASH with fibrosis (Table 1) [41]. In the subgroup of 79 patients whose adipose tissues were available 16 were classified as MHO with normal liver (20 %) and n = 63 (80 %) as MUHO with MASLD (Fig. 1**;** Table 2).

### 3.2. Gene signature, pathway-enriched and networks which features MASLD

In the attempt to identify liver and adipose-related genes which may allow to feature MASLD in obese patients with metabolic alterations, we performed a differential analysis comparing MUHO to MHO. In hepatic tissue, there were 498 significant DEGs (n = 208 upregulated and n = 290 downregulated; p-adj < 0.05) in MUHO, the most upregulated were those involved in lipid droplets assembly and metabolism (*CIDEC, LPL, FNDC5*), TGFβ signaling (*SMAD5, TSPAN3*), glycolytic pathway and insulin resistance (*ENO3, PRKAA2*), mitophagy (*OPTN*) and those which exhibited proliferation and survival significance (*ZBTB33, TNK2, PLXNA4, TRPV4)*. Conversely, the expression of genes related to glucose, insulin (*IGF1, GPC3, ITLN1*) and lipid dismissal (*APOF*), mitochondrial function (*ALDH6A1, KARS1, NDUFB1, SOD1*), hepatocyte regeneration (*FGL1*) as well as that of a long noncoding RNA (*DIO3OS*) which suppresses termogenesis was strongly reduced (Table 3, Fig. 2**A**).

In adipose tissue, we revealed 189 DEGs in MUHO *vs* MHO

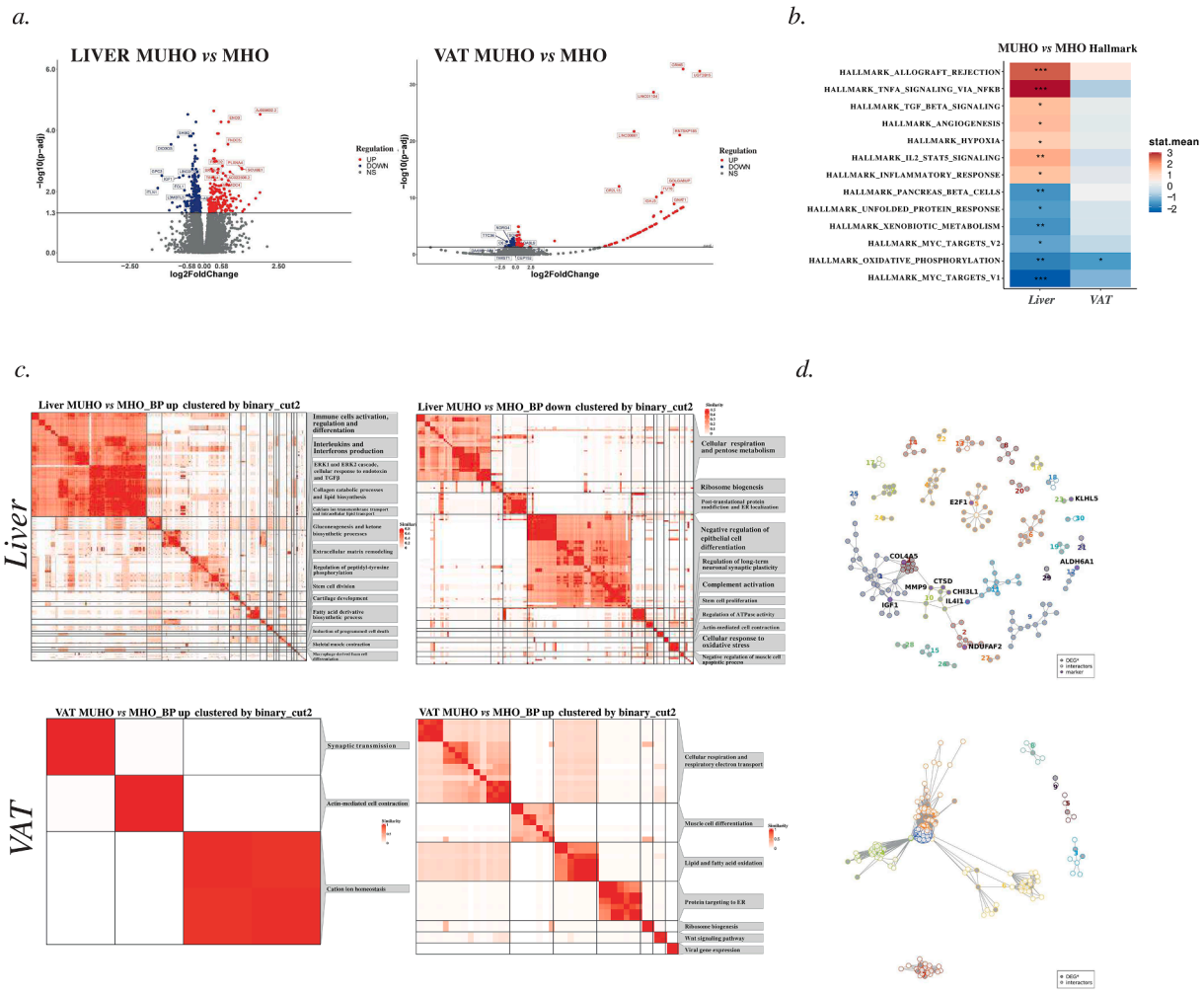


**Fig. 2.** Gene signature which features MUHO patients in liver and adipose tissue. Volcano plots illustrate the differentially expressed genes (DEGs) observed in the MUHO *vs* MHO comparison in both liver and adipose tissue. X-axis shows the log2 fold change, whereas y-axis represents the negative logarithmic (-log10) of *p*-value adjusted (p-adj). Significantly downregulated DEGs are plotted in blue, upregulated DEGs in red, and non-significant DEGs in dark grey. The continuous line indicates the threshold of p-adj $< 0.05$ above which significant DEGs are plotted (A). Pathway-enriched analysis of DEGs in the comparison MUHO *vs* MHO by using HALLMARK in the liver (on the left) and in adipose tissue (on the right). Red shading indicates induction and blue shading indicates repression relative to the stat. mean (mean of gene set test statistics). *p $< 0.1$, **p $< 0.05$, ***p $< 0.01$ (B). Gene ontology (GO)-terms of the category biological processes (BP), in which DEGs are involved, is clustered according to their similarity employing the binary cut method. Heatmaps illustrate the GO-BP-terms upregulated (on the left) and down-regulated (on the right) that clustered together by similarity index in the liver (on top) and the adipose tissue (on bottom) (C). Networks enriched in DEGs in liver (on top) and adipose tissue (on bottom); the numbers indicate the topological communities; nodes: genes; links: molecular interactions from STRING (D).

**Table 4**
List of the main VAT up- and dowregulated coding and non-coding genes in the comparison MUHO *vs* MHO.

| **Upregulated** | | | **Down-regulated** | | |
|---|---|---|---|---|---|
| **Genes** | **p-value** | **p-adj** | **Genes** | **p-value** | **p-adj** |
| GRM5 | 5.7E-38 | 1.8E-33 | TTC36 | 1.2E-05 | 0.005 |
| UGT2B15 | 2.6E-37 | 4.2E-33 | NDRG4 | 1.5E-05 | 0.006 |
| OR2L13 | 2.0E-16 | 9.4E-13 | NDUFB10 | 4.1E-05 | 0.01 |
| FUT6 | 3.1E-15 | 1.2E-11 | CIDEA | 5.8E-05 | 0.01 |
| GNAT1 | 3.7E-13 | 1.2E-09 | C6 | 8.6E-05 | 0.02 |
| PRDM12 | 1.8E-12 | 4.9E-09 | COQ8A | 0.0001 | 0.03 |
| MOGAT3 | 3.2E-12 | 7.4E-09 | CA3 | 0.0001 | 0.03 |
| PANX3 | 8.9E-11 | 1.4E-07 | TWIST1 | 0.0001 | 0.03 |
| CCL1 | 1.4E-08 | 1.4E-05 | PCK2 | 0.0002 | 0.04 |
| ALPP | 3.8E-08 | 3.4E-05 | IGF1 | 0.0002 | 0.04 |
| **Non-coding** | **p-value** | **p-adj** | **Non-coding** | **p-value** | **p-adj** |
| LINC01104 | 2.0E-33 | 2.2E-29 | SNHG29 | 8.9E-06 | 0.004 |
| LINC00661 | 2.3E-26 | 1.9E-22 | APTR | 7.9E-05 | 0.02 |
| RN7SKP185 | 1.3E-25 | 8.4E-22 | DAAM2-AS1 | 0.0001 | 0.03 |

comparison (n = 127 upregulated and n = 62 downregulated). The expression of those involved in lipid-glucose metabolism (*UGT2B15, FUT6, LEP, VLDLR*), glutamate receptors (*GRM5*), regulators of adipose tissue mass (*OR2L13, PRDM12, GNAT1, MOGAT3, ALPP, PANX3*) inflammation (*CCL1, IGTB5*) and calcium sensing (*CALM1*) was significantly higher, whereas the most downregulated were genes related to apoptosis (*NDRG4, TTC36, GLYCTK*), TCA cycle and mitochondrial respiratory chain (*NDUFB10, PCK2* and *COQ8A*), metabolic healthy phenotype (*CIDEA, TWIST1*). Among the downregulated DEGs, we found *CA3*, whose inhibition induces adipocytes differentiation, and *C6* which belong to the complement cascade (Table 4; Fig. 2**A**).

By using the integrated database OmniPath we inferred ligand-receptor interactions between liver and VAT among DEGs with a p-adjusted $< 0.05$. Specifically, the upregulated *FNDC5*, *PRKAA2*, *LPL* and *TRPV4* genes in hepatic tissue from MUHO patients were predicted to interact with *ITGB5*, *LEP*, *VLDLR* and *CALM1* in VAT, respectively. FNDC5 and LPL are released from the liver and bind to the membrane proteins ITGB5 and VLDLR in VAT with a strength of interaction of 10.7 and 10.2 whereas LEP is secreted from adipose tissue and interact with PRKAA2 in the liver showing a score of 7.1. Neither TRPV4 in the liver

**Table 5**
List of DEGs derived from the Ligand-Receptor interactions analysis between liver and VAT by comparing MUHO *vs* MHO.

| Gene1 origin | Gene1 | Gene1 secreted | Gene1 origin | Gene2 | Gene2 secreted | L-R score | p-adj < 0.01 | p-adj < 0.05 |
|---|---|---|---|---|---|---|---|---|
| Liver | FNDC5 | yes | Adipose | ITGB5 | no | 10.7 | yes | yes |
| Liver | PRKAA2 | no | Adipose | LEP | yes | 7.1 | yes | yes |
| Liver | LPL | yes | Adipose | VLDLR | no | 10.2 | yes | yes |
| Liver | TRPV4 | no | Adipose | CALM1 | no | 3.6 | yes | yes |

nor CALM1 in adipose tissue are secreted proteins and their interaction score is lower than the others (score = 3.6) possibly suggesting that their crosstalk may be mediated by other proteins. These inferred interactions between genes previously described to be upregulated during MASLD confirmed the relevance of liver-VAT crosstalk in disease onset in metabolically unhealthy status (Table 5).

Next, we performed pathway-enriched analysis on protein-coding genes in hepatic and adipose tissue by comparing MUHO *vs* MHO. According to HALLMARK dataset, the hepatic upregulated pathways enriched in MASLD included TNF α signaling (JUN, cytokines and

**Table 6**
List of communities derived from network analysis in liver by comparing MUHO *vs* MHO.

| comm_id | size | gsid | p | p_adj |
|---|---|---|---|---|
| 1 | 27 | HALLMARK_EMT | 0.00054574 | 0.0272872 |
| 1 | 27 | HALLMARK_COAGULATION | 0.00259063 | 0.0647657 |
| 1 | 27 | HALLMARK_HYPOXIA | 0.00641031 | 0.0851111 |
| 1 | 27 | HALLMARK_GLYCOLYSIS | 0.00680888 | 0.0851111 |
| 2 | 8 | HALLMARK_OXIDATIVE_PHOSPHORYLATION | 4.64E-08 | 2.32E-06 |
| 2 | 8 | HALLMARK_ADIPOGENESIS | 0.00485961 | 0.1214902 |
| 2 | 8 | HALLMARK_FATTY_ACID_METABOLISM | 0.08806234 | 1 |
| 3 | 10 | HALLMARK_EMT | 1.34E-07 | 6.68E-06 |
| 3 | 10 | HALLMARK_HYPOXIA | 0.00837196 | 0.1091561 |
| 3 | 10 | HALLMARK_MYOGENESIS | 0.0086417 | 0.1091561 |
| 3 | 10 | HALLMARK_GLYCOLYSIS | 0.00873248 | 0.1091561 |
| 3 | 10 | HALLMARK_ANGIOGENESIS | 0.02636426 | 0.2636426 |
| 4 | 9 | HALLMARK_MYOGENESIS | 7.14E-08 | 3.57E-06 |
| 4 | 9 | HALLMARK_EMT | 0.12143724 | 1 |
| 5 | 14 | HALLMARK_G2M_CHECKPOINT | 0.01841362 | 0.9206811 |
| 5 | 14 | HALLMARK_PI3K_AKT_MTOR_SIGNALING | 0.10841119 | 1 |
| 5 | 14 | HALLMARK_HEME_METABOLISM | 0.15655046 | 1 |
| 5 | 14 | HALLMARK_MYC_TARGETS_V1 | 0.19511032 | 1 |
| 6 | 10 | HALLMARK_FATTY_ACID_METABOLISM | 0.00016653 | 0.0068716 |
| 6 | 10 | HALLMARK_ADIPOGENESIS | 0.00027486 | 0.0068716 |
| 6 | 10 | HALLMARK_CHOLESTEROL_HOMEOSTASIS | 0.00119188 | 0.0198646 |
| 6 | 10 | HALLMARK_PEROXISOME | 0.00223304 | 0.0228116 |
| 6 | 10 | HALLMARK_BILE_ACID_METABOLISM | 0.00228116 | 0.0228116 |
| 6 | 10 | HALLMARK_MTORC1_SIGNALING | 0.00900745 | 0.0750621 |
| 6 | 10 | HALLMARK_ANGIOGENESIS | 0.02636426 | 0.1883161 |
| 7 | 7 | HALLMARK_ALLOGRAFT_REJECTION | 0.00011614 | 0.0058071 |
| 7 | 7 | HALLMARK_IL6_JAK_STAT3_SIGNALING | 0.04629228 | 0.8024153 |
| 7 | 7 | HALLMARK_TNFA_SIGNALING_VIA_NFKB | 0.09427343 | 0.8024153 |
| 7 | 7 | HALLMARK_HYPOXIA | 0.09528211 | 0.8024153 |
| 7 | 7 | HALLMARK_INFLAMMATORY_RESPONSE | 0.09578609 | 0.8024153 |
| 8 | 6 | HALLMARK_DNA_REPAIR | 0.06679677 | 1 |
| 8 | 6 | HALLMARK_G2M_CHECKPOINT | 0.08749139 | 1 |
| 8 | 6 | HALLMARK_E2F_TARGETS | 0.0901055 | 1 |
| 9 | 14 | HALLMARK_UNFOLDED_PROTEIN_RESPONSE | 0.0060561 | 0.2369555 |
| 9 | 14 | HALLMARK_HEME_METABOLISM | 0.01199743 | 0.2369555 |
| 9 | 14 | HALLMARK_MTORC1_SIGNALING | 0.01752419 | 0.2369555 |
| 9 | 14 | HALLMARK_MYC_TARGETS_V1 | 0.01895644 | 0.2369555 |
| 9 | 14 | HALLMARK_WNT_BETA_CATENIN_SIGNALING | 0.04517603 | 0.4517603 |
| 10 | 8 | HALLMARK_KRAS_SIGNALING_UP | 0.00427437 | 0.2137183 |
| 10 | 8 | HALLMARK_COAGULATION | 0.07933921 | 0.5249652 |
| 10 | 8 | HALLMARK_P53_PATHWAY | 0.09958065 | 0.5249652 |
| 11 | 12 | HALLMARK_XENOBIOTIC_METABOLISM | 1.56E-05 | 0.0007796 |
| 11 | 12 | HALLMARK_FATTY_ACID_METABOLISM | 0.00797589 | 0.1993972 |
| 11 | 12 | HALLMARK_KRAS_SIGNALING_UP | 0.14234259 | 1 |
| 11 | 12 | HALLMARK_MTORC1_SIGNALING | 0.16337427 | 1 |
| 12 | 4 | HALLMARK_OXIDATIVE_PHOSPHORYLATION | 0.00141109 | 0.0705546 |
| 12 | 4 | HALLMARK_UNFOLDED_PROTEIN_RESPONSE | 0.03346594 | 0.7910312 |
| 12 | 4 | HALLMARK_HEME_METABOLISM | 0.04746187 | 0.7910312 |
| 13 | 6 | HALLMARK_BILE_ACID_METABOLISM | 0.00077499 | 0.0387497 |
| 13 | 6 | HALLMARK_PEROXISOME | 0.04253862 | 0.9841553 |
| 13 | 6 | HALLMARK_ADIPOGENESIS | 0.07873242 | 0.9841553 |
| 14 | 5 | HALLMARK_TGF_BETA_SIGNALING | 0.01984836 | 0.7198 |
| 14 | 5 | HALLMARK_KRAS_SIGNALING_DN | 0.0597205 | 0.7198 |
| 14 | 5 | HALLMARK_GLYCOLYSIS | 0.07050085 | 0.7198 |
| 14 | 5 | HALLMARK_MITOTIC_SPINDLE | 0.07198 | 0.7198 |
| 15 | 3 | HALLMARK_CHOLESTEROL_HOMEOSTASIS | 0.0156869 | 0.3921726 |
| 20 | 3 | HALLMARK_DNA_REPAIR | 0.0339716 | 1 |

**Table 7**
List of communities derived from network analysis in VAT by comparing MUHO *vs* MHO.

| comm_id | size | gsid | p | p_adj |
|---|---|---|---|---|
| **1** | **77** | **HALLMARK_COMPLEMENT** | **0.02558639** | **1** |
| 1 | 77 | HALLMARK_COAGULATION | 0.04477658 | 1 |
| 1 | 77 | HALLMARK_INFLAMMATORY_RESPONSE | 0.09759275 | 1 |
| 1 | 77 | HALLMARK_PI3K_AKT_MTOR_SIGNALING | 0.13037784 | 1 |
| 2 | 112 | HALLMARK_INFLAMMATORY_RESPONSE | 5.58E-07 | 2.79E-05 |
| 2 | 112 | HALLMARK_APOPTOSIS | 0.04766414 | 0.60749692 |
| 2 | 112 | HALLMARK_KRAS_SIGNALING_DN | 0.04859975 | 0.60749692 |
| 2 | 112 | HALLMARK_PI3K_AKT_MTOR_SIGNALING | 0.06359257 | 0.63592569 |
| 3 | 7 | HALLMARK_PANCREAS_BETA_CELLS | 3.25E-12 | 1.63E-10 |
| 3 | 7 | HALLMARK_KRAS_SIGNALING_DN | 0.08260409 | 1 |
| 4 | 30 | HALLMARK_MITOTIC_SPINDLE | 0.07256709 | 1 |
| 4 | 30 | HALLMARK_PEROXISOME | 0.19551676 | 1 |
| 5 | 5 | HALLMARK_IL6_JAK_STAT3_SIGNALING | 0.03328646 | 1 |
| 5 | 5 | HALLMARK_XENOBIOTIC_METABOLISM | 0.06679472 | 1 |
| 5 | 5 | HALLMARK_COMPLEMENT | 0.07050085 | 1 |
| 6 | 29 | HALLMARK_ANGIOGENESIS | 0.00267998 | 0.13399906 |
| 6 | 29 | HALLMARK_ADIPOGENESIS | 0.0069274 | 0.17318492 |
| 6 | 29 | HALLMARK_HEME_METABOLISM | 0.04759086 | 0.48146169 |
| 6 | 29 | HALLMARK_APOPTOSIS | 0.04814617 | 0.48146169 |
| 7 | 22 | HALLMARK_GLYCOLYSIS | 0.00025603 | 0.01280127 |
| 7 | 22 | HALLMARK_TNFA_SIGNALING_VIA_NFKB | 0.03768572 | 0.71389551 |
| 7 | 22 | HALLMARK_NOTCH_SIGNALING | 0.05384018 | 0.71389551 |
| 8 | 6 | HALLMARK_XENOBIOTIC_METABOLISM | 0.00271101 | 0.13555036 |
| 8 | 6 | HALLMARK_FATTY_ACID_METABOLISM | 0.06679677 | 0.59371872 |
| 8 | 6 | HALLMARK_APOPTOSIS | 0.07078956 | 0.59371872 |
| 8 | 6 | HALLMARK_TNFA_SIGNALING_VIA_NFKB | 0.08136744 | 0.59371872 |

chemokines), angiogenesis, inflammatory response, TGFβ signaling (SMAD, TGFβ) and hypoxia. Conversely, the downregulated ones were MYC Targets V1, xenobiotic metabolism (cytochrome pathway), oxidative phosphorylation (NDUF, COX, OXA1L) and unfolded protein response (UPR) (Fig. 2**B**). As an independent confirmatory approach, we also performed the enrichment analysis using KEGG gene sets resulting in very similar processes.

In adipose tissue, HALLMARK analysis highlighted oxidative phosphorylation (NDUF, COX, UQCR) as the only de-regulated (down) pathway in the MUHO *vs* MHO comparison (Fig. 2**B**). Conversely, KEGG gene sets provided as upregulated the glycosphingolipid biosynthesis lacto and neolacto series, carbohydrate metabolism (ENPP, G6PC, GAA, UGTs), calcium signaling, whereas among the downregulated we found fatty acid metabolism (CPT1, ACAT1 and ACAT2), ribosome and mitochondrial-ribosome assembly.

Therefore, oxidative phosphorylation results the only significantly downregulated pathway both in liver and adipose tissue during MASLD. In keeping with this observation, a reduced mitochondrial respiration in VAT has been recently associated with insulin resistance and inflammation thus discriminating obese patients who develop MASLD from those who do not [4].

In addition, we also performed GAGE analysis using the Gene Ontology (GO) to explore the functional roles of protein-coding genes. In the liver, the key biological processes that were upregulated in MUHO *vs* MHO were mainly involved in immune system activation, leukocytes chemotaxis, interleukins, ERK1/2 cascade, cytoskeleton reorganization, cellular response to TGFβ, collagen synthesis, regulation of lipid biosynthesis, intracellular lipid transport, gluconeogenesis and ketonegenesis (Fig. 2**C**, upper panel). Among the downregulated ones we found processes related to respiratory ETC, pentose metabolism, post-translational protein modifications, protein localization to endoplasmic reticulum (ER), response to oxidative and ER stress, ATPase activity, response to UPR and complement activation (Fig. 2**C**, upper panel).

In adipose tissue, there were mostly downregulated biological processes among which cellular respiration, respiratory ETC, fatty acid and lipid oxidation, protein targeting to ER and ribosome/mitoribosome biogenesis (Fig. 2**C** lower panel). Overall, GO further corroborated the pathway-enriched analysis, supporting the role of mitochondrial failure in VAT during the onset of obesity-related complications and MASLD.

Finally, a protein–protein network for DEGs was generated to identify communities, i.e. groups of genes that establish more interactions within the community than outside of it, thus reflecting distinct biological functions. In the liver, by analyzing MUHO *vs* MHO, we found a network of 178 proteins organized in 30 communities. The largest were related to epithelial mesenchymal transition (EMT), glycolysis and hypoxia, followed by those linked to PI3K-AKT-MTOR signaling, UPR, adipogenesis, cholesterol and bile acid homeostasis (Fig. 2**D**). Topological analysis showed that IGF1 has the highest degree and betweenness in MUHO *vs* MHO in hepatic tissue, possibly suggesting a key biological function of this protein (Fig. 2**D**).

In adipose tissue, we found 9 communities including 290 proteins. The largest were related to inflammatory response, complement activation, coagulation and PI3K-AKT-MTOR signaling. The smallest ones included pathways involved in apical junction, glycolysis, TNF α signaling and adipogenesis. Topological analysis demonstrated that MOGAT3, a putative triacyglycerol synthase has the highest degree and betweenness in MUHO *vs* MHO, confirming its association with adipose tissue metabolic abnormalities [42] (Fig. 2**D,** Tables 6 and 7).

### 3.3. Comparative analysis of DEGs to identify possible disease biomarkers

To identify the Genes of Interest (GoI) which may feature MASLD and that might be possibly used as specific biomarkers of metabolically unhealthy obesity, we performed a comparative analysis of DEGs between hepatic and adipose tissues. In MUHO *vs* MHO we found 5 DEGs shared by the two tissues (Fig. 3**A**). Out of them, four genes were downregulated (*C6, IGF1, OXA1L, NDUFB11*) whereas *KLHL5* was upregulated (Fig. 3**B**).

C6 is a protein of the complement system, IGF-1 induces insulin sensitivity and shows anti-fibrotic properties in *in vivo* models of MASH. Indeed, low IGF-1 levels have been associated with hepatic fat accumulation, inflammation and fibrosis in obese subjects and it might be a useful biomarker to discriminate advanced fibrosis [43,44]. OXA1L is localized in the inner mitochondrial membrane and it is involved in the gathering of the cytochrome *C* oxidase and ATPase complexes of the mitochondrial respiratory chain. Its downregulation may impair mitochondrial biogenesis and ATP synthesis. NDUFB11 is a subunit of NADH

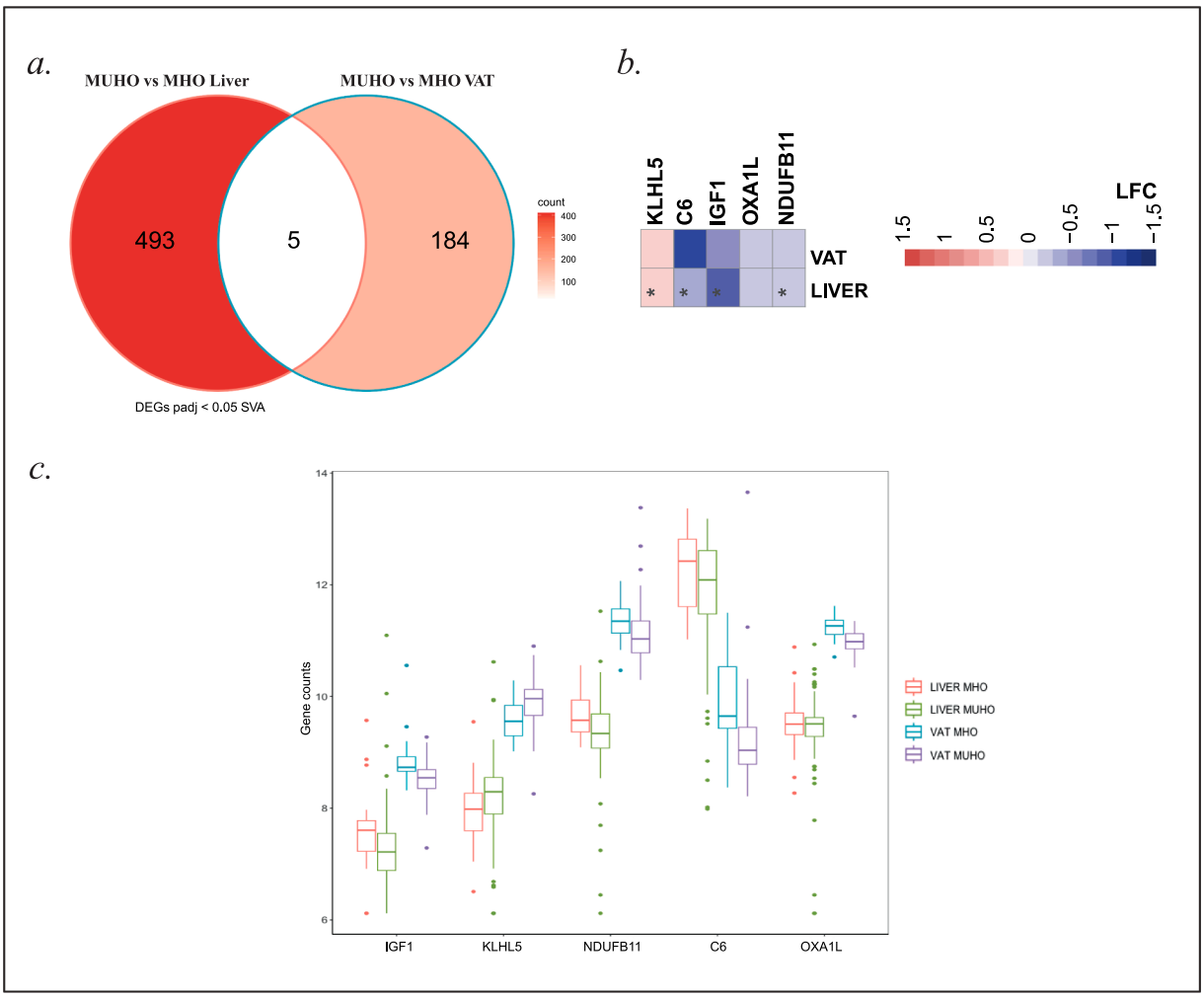


**Fig. 3.** Comparative analysis of DEGs to identify a specific gene signature. Venn diagram is exploited to identify the 5 common DEGs (padj < 0.05) in MUHO *vs* MHO comparison, shared by liver and adipose tissue (A). Heatmap illustrates the expression of each DEG across MUHO and MHO status in both tissues. Red and blue shading indicate induction and repression, respectively. KLHL5 and C6 genes belong to the immune system pathway, IGF1 to the PI3K-AKT-MTOR signaling whereas OXA1L and NDUFB11 to the oxidative phosphorylation pathway (B). The expression of 5 common genes between liver and adipose tissue in MUHO *vs* MHO comparison is stratified according to the presence of MASLD in both liver (on the left) and adipose tissue (on the right). Boxes span from 25° to 75° percentile, while whiskers indicate the 10° and 90° percentile. MHO is plotted in red, while MUHO in blue (C).

dehydrogenase complex I, which participates to the ETC in mitochondria. *KLHL5* expression has been found upregulated in gastric cancer and correlated with poorer overall survival. The differential expression of these genes between MUHO *vs* MHO was even more striking in adipose tissue (Fig. 3**C**). Accordingly, at ROC curve, the adipose tissue expression of C6, IGF1 and OXA1L genes have a higher specificity in prediciting MASLD compared to the hepatic ones (Fig. 4**A-E**). This results support the importance of a different transcriptional phenotype in MUHO than MHO subjects and the enormous contribution of dysfunctional VAT in promoting the onset of MASLD.

Notably, the diagnostic accuracy of each gene expression in predicting the presence MASLD in MUHO increased combining all 5 genes (AUC = 0.82 liver; AUC = 0.89 adipose) (Fig. 5**A**). These results suggest that the simultaneous assessment of *C6, IGF1, OXA1L, NDUFB11* and *KLHL5* which are genes shared by the liver and adipose tissue may help to distinguish MHO from MUHO individuals were the latter are predisposed to develop progressive MASLD and related-comorbidities.

In the attempt to translate RNA sequencing in clinical diagnostic, we assessed serum levels of C6 and IGF1, which are the only secreted proteins among those included in the gene signature, in 15 MHO and 37 MUHO patients.

Both C6 and IGF1 circulating proteins were significantly lower in MUHO subjects compared to MHO (p = 0.0009; p = 0.006) thus confirming transcriptomic data and suggesting their use as potential biomarkers for the detection of unhealthy status in obese individuals (Fig. 5**B**). At multivariate analysis adjusted for age, gender, T2D and BMI, C6 and IGF-1 remained significantly associated with the unhealthy status (beta = -6.11, CI:-12.7–2.64, p = 0.01; beta = -1.60, CI:-3.20–0.50, p = 0.015). Moreover, at ROC analysis the combined assessment of circulating C6 and IGF-1 has a diagnostic accuracy of 0.87 in diagnosisng MUHO (Fig. 5**B**).

### 3.4. Validation of candidate genes in differentiated adipocytes isolated from human VAT

Finally, we decided to validate the altered epression of *C6, IGF1, OXA1L, NDUFB11* and *KLHL5* genes in hepatic samples and in primary adipocytes isolated from 12 matched VAT specimens, stratified according to the presence of unhealthy obesity and MASLD. We observed that the mRNA levels of *C6, IGF1, OXA1L, NDUFB11* were strongly reduced, while that of *KLHL5* was upregulated, thus mirroring transcriptomic results (Fig. 5**C-D**).

Western blot analysis was performed in hepatic samples and primary adipocytes from obese patients stratified according to the MHO (n = 6)

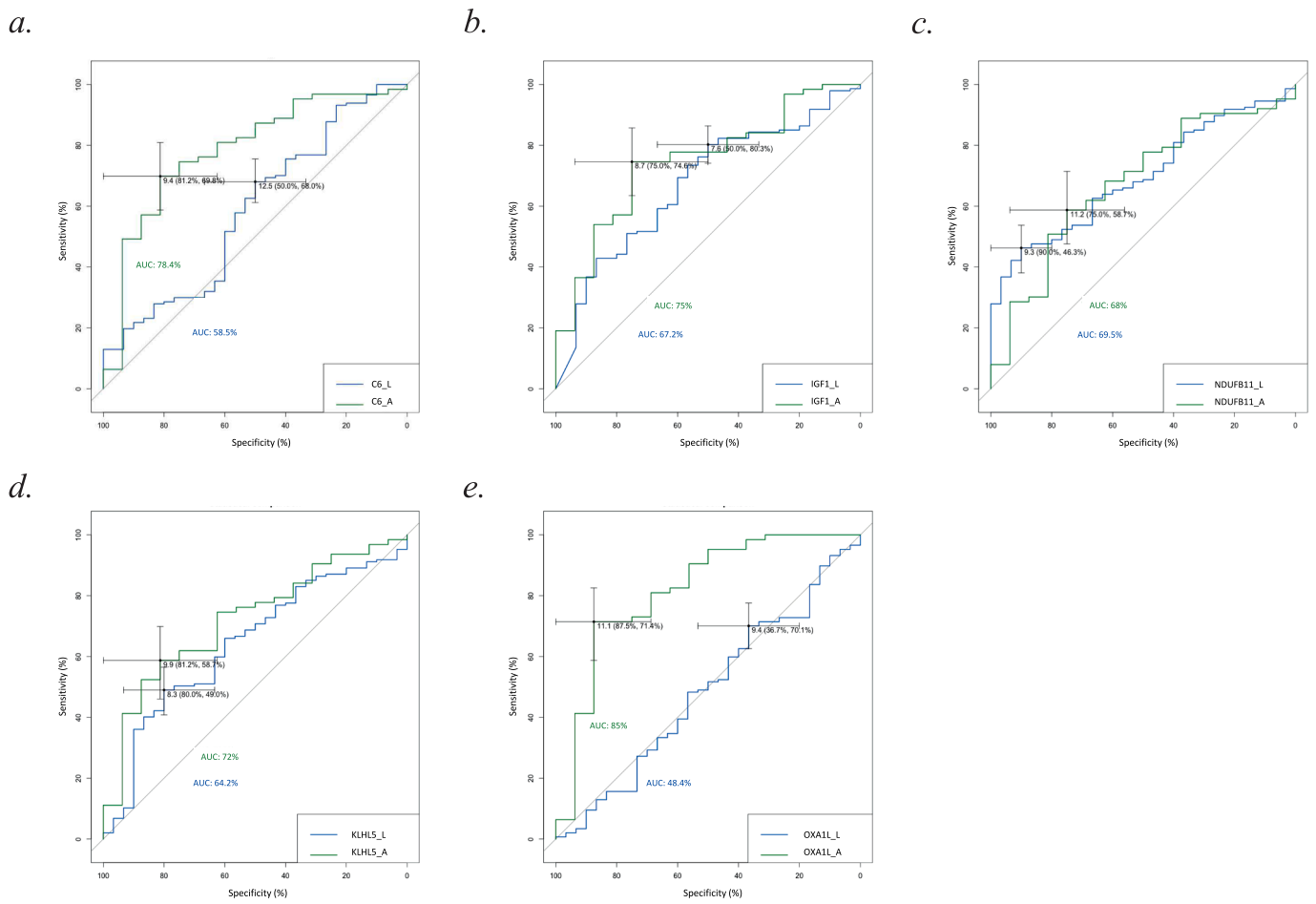


**Fig. 4.** Comparison between the accuracy of 5 common genes deregulated in both liver and VAT in discriminating MASLD. ROC curves describe the accuracy of hepatic (blue line) and adipose tissue (green line) gene expression of C6 (A), IGF1 (B), NDUFB11 (C), KLHL5 (D), (E), OXA1L (F) and in foreseeing MASLD in metabolic unhealthy obese (MHUO) individuals. Area under the curves (AUC) are reported in the graphs.

and MUHO (n = 6) classification. We confirmed that protein levels of OXA1L, NDUFB11 were reduced wheresas those of KLHL5 were higher in hepatic and VAT samples obtained from MUHO patients (Fig. 5**E-F**).

## 4. Discussion

In this study, we compared the hepatic and adipose tissue transcriptomic profiles in metabolically healthy and unhealthy obese individuals with the purpose to identify specific pathways and gene signatures which participate to the onset of MASLD in the presence of metabolic dysfunctions in MUHO.

We performed an high throughput RNA sequencing of 167 hepatic samples and 79 matched adipose tissues derived from adult patients with severe obesity, who underwent bariatric surgery to manage overweight and reduce the risk of obesity-related comorbidities, including MASLD. According to the Wildman definition [41], we stratified patients in metabolically healthy (MHO) and unhealthy (MUHO) characterized by the presence of glucose intolerance/T2D, higher cardiovascular risk and MASLD, although sharing the same grade of adiposity with MHO.

Firstly, we performed a differential analysis comparing the two categories of patients and we found 498 significant DEGs in liver (208 up and 290 down) and 189 in adipose tissue (127 up and 62 down). The most upregulated genes in both tissues in MUHO were those related to inflammation and lipid metabolism whereas the expression of genes involved in insulin signaling and mitochondrial function was reduced.

Similarly, pathway and network analyses in the liver confirmed an upregulation of inflammation, TNF α /TGFβ signaling, hypoxia and a reduction of PI3K signaling and oxidative phosphorylation in MUHO compared to MHO. Mitochondrial respiration was downregulated also in adipose tissue thus confirming recent findings which described how VAT mitochondrial function was impaired in MASH obese patients compared to those without liver disease. In addition, the failure of mitochondrial respiration in VAT was associated with local inflammation and IR [4]. Therefore, as previously reported the MUHO definition implies a pro-inflammatory status characterized by a transcriptional activation of TNF α, which in turn amplifies IR and inhibits OXPHOS complexes [45,46].

Moreover, the results obtained by the previous analyses were corroborated by Gene Ontology which demonstrated that the main downregulated biological processes in MUHO were involved in respiratory electron transport chain, lipid oxidation, protein targeting to ER and ribosomal/mitoribosomal biogenesis, showing not only a reduced cellular respiration, but also an impairment of ribosome and mitochondrial-ribosome assembly. An abnormal expression of mitochondrial ribosomal genes fosters metabolic disorders including MASLD and they have been associated with several mitochondrial diseases [47,48]. All these results corroborate the emerging evidence according to which the enhancement of oxidative phosphorylation, mitochondrial biogenesis and mitophagy with the subsequent removal of toxic lipid species could be druggable as recently demonstrated by the completed clinical studies which pointed Resmetirom as a novel leader in the crowded field of MASH therapeutics [49].

Next, to identify genes which may feature the metabolic unhealthy status we performed a comparative DEGs analysis revealing 5 genes

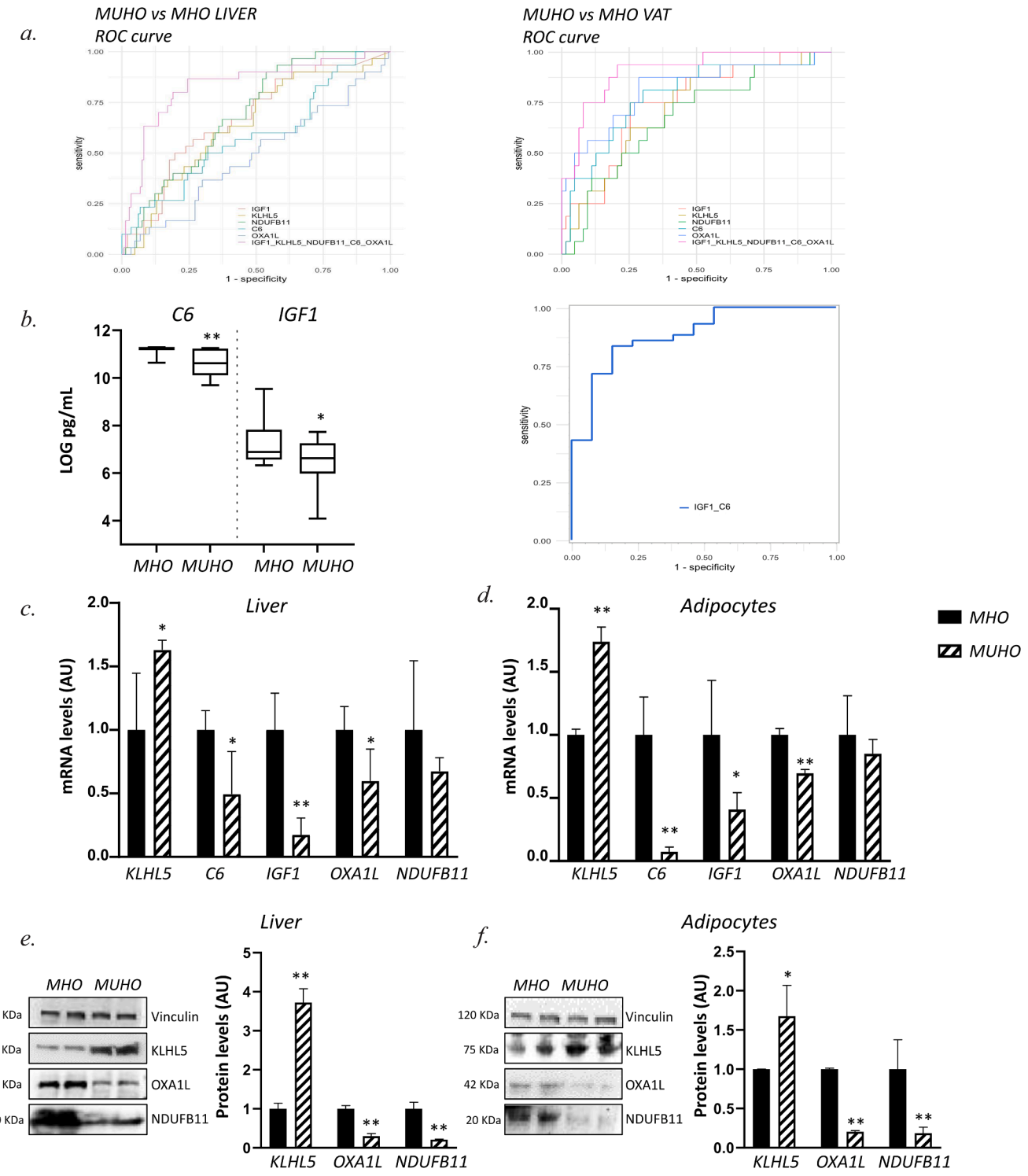


**Fig. 5.** Diagnostic accuracy of the 5-genes signature in predicting the onset of MASLD in MUHO individuals ROC curves of 5 common DEGs (padj < 0.05) in MUHO *vs* MHO comparison shared by liver (on the left) and adipose tissue (on the right), obtained considering each gene alone, or 5 genes combined in a generalized linear model (A). Circulating levels of C6 and IGF-1 were assessed in 52 serum samples (15 MHO and 37 MUHO) by ELISA. ROC curve of serum C6 and IGF-1 in MUHO *vs* MHO comparison by combining them in a generalized linear model (B). The expression of *KLHL5*, *C6*, *IGF1*, *OXA1L* and *NDUFB11* has been was evaluated by qRT-PCR in livers (on the left) and in primary adipocytes (on the right) isolated from n = 12 bariatric patients, stratified according to MHO and MUHO classification; mRNA levels were normalized to β-actin. Data are expressed as fold increase compared to MHO (C-D). Protein levels of *KLHL5*, *OXA1L* and *NDUFB11* have been was evaluated by Western Blotting in hepatic samples (on the left) and in primary adipocytes (on the right); stratified according to the MHO (n = 6) and MUHO (n = 6) classification. Protein levels were quantified by ImageJ software (National Institutes of Health, Bethesda, MD) and normalized to vinculin as housekeeping gene (E-F). At least 3 independent experiments were conducted. ** $p < 0.001$, * $p < 0.05$ according to Student's *t*-test.

commonly deregulated in both hepatic and adipose tissues. *C6*, *IGF1*, *OXA1L* and *NDUFB11* were downregulated whereas *KLHL5* expression was increased, and their alterations were even more noticeable in adipose tissue, sustaining its relevance in MASLD initiation in unhealthy obese subjects. According to the previously mentioned impaired mitochondrial function in MUHO, *OXA1L* and *NDUFB11* genes codify for proteins both localized in the inner membrane. Specifically, the Oxidase (Cytochrome *C*) Assembly 1-like (OXA1L) is a translocase, involved in the gathering of the cytochrome *C* oxidase and ATPase complexes of the mitochondrial respiratory chain. OXA1L downregulation may impair mitochondrial biogenesis, ATP synthesis and mitochondrial ribosome packaging, whereby reducing the anchoring mitoribosomes to the mitochondrial inner membrane. Conversely, the NADH: ubiquinone oxidoreductase subunit B11 (NDUFB11) is a subunit of NADH dehydrogenase complex I, which participates to the electron transport chain in mitochondria. It has been reported that both genes were downregulated in adipose tissue isolated from patients affected by acquired-obesity thus suggesting an impairment of mitochondrial biogenesis and a defective mitochondrial function [50].

Among the 5-genes signature, we found also the Insulin-like growth factor 1 (IGF-1), an hormone which ensures insulin sensitivity and shows anti-fibrotic properties in *in vivo* models of MASH. Interestingly, according to topological analysis, we also demonstrated that IGF1 displayed the highest degree and betweenness in the comparison MUHO *vs* MHO, possibly suggesting a key biological function of this protein. Indeed, it participates in the differentiation of preadipocytes and regulates lipid storage capacity and adipose tissue mass, in physiological conditions [51]. Therefore, it might be speculated that aberrancies in its transcriptomal profile could predispose to the development of a metabolic unhealthy phenotype, impeding adipose tissue expansion and fostering in turn fatty acid release and IR [52]. In keeping with this notion, low IGF-1 levels have been previously associated with hepatic fat accumulation, inflammation and fibrosis in obese subjects, even representing an useful biomarker to discriminate advanced fibrosis [43,44].

Among the other genes in the signature we found *C6* belonging to the complement system and Kelch Like Family Member 5 (*KLHL5*). The former combines with C5b, C7, C8 e C9 to form the membrane attack complex (MAC), playing a key role in the immune response by assembling transmembrane channels which disrupt the membrane of target cells, leading to their lysis and death [53]. The latter, has been found upregulated in gastric cancer and correlated with poorer overall survival and high infiltration levels. KLHL family genes are noted for their involvement in the E3 ligase ubiquitination pathway and *KLHL5* knockdown decreased the viability of cancer cells and sensitized them to numerous anti-cancer drugs [54].

Overall, this 5-gene signature, obtained by the combined assessment of transcriptomic profiles of hepatic and adipose tissue in the context of obesity, may constitute a novel tool to discriminate MHO subjects from MUHO, who have the higher risk to develop advance disease. In particular, we outlined the importance of a different transcriptional phenotype between metabolic unhealthy and healthy obese in promoting MASLD and metabolic disturbances. Accordingly, at both univariate and multivariate analysis, serum levels of C6 and IGF-1 were reduced in MUHO thus suggesting their assessment as circulating biomarkers for the definition of unhealthy status in obese individuals.

Finally, to corroborate the findings drawn by transcriptomic data, we confirmed the expression pattern of the 5-gene signature also in another small cohort of bariatric patients from whom hepatic biopsies and matched primary adipocytes differentiated from mesenchymal stem cells have been collected.

The first limitation of the study is represented by the low number of obese patients included in the MHO group although it is aligned with literature data (~10–15 %) [55]. Secondly, we cannot exclude the presence of pre-diabetes in MHO patients since they didn't undergo oral glucose tolerant test (OGTT). Anyway, HbA1c and fasting glucose levels fall in normal ranges for all MHO patients, thus possibly ruling out a IGT status.

To sum up, our study identified for the first time, the main dysfunctional pathways and the specific transcriptomic signature which may connect both liver and VAT during the onset of MASLD in the context of severe overweight. This signature may be decisive in triggering the onset of obesity-related complications by turning metabolic healthy individuals into unhealthy ones, albeit they share the same grade of adiposity. Therefore, it constitutes a good opportunity to further address our efforts in the discovery of biomarkers that may integrate the scant performance of non-invasive score in the context of obesity.

## 5. Financial support

This study was supported by Italian Ministry of Health (Ricerca Corrente 2023 - Fondazione IRCCS Cà Granda Ospedale Maggiore Policlinico), by Italian Ministry of Health (Ricerca Finalizzata Ministero della Salute GR-2019–12370172; RF-2021–12374481) and by 5X1000 2020 Fondazione IRCCS Cà Granda Ospedale Maggiore Policlinico, RC5100020B.

## 6. Contributors

The authors' responsibilities were as follows: MMe, study design, data analysis and interpretation, manuscript drafting; EDc, FC, EM, IM, AO, AM data analysis and interpretation; EP and ML data generation; RL, SB and MMa patients enrollment; LVC, ALF revised the manuscript; PD study design, manuscript drafting, data analysis and interpretation, study funding, supervision and has primary responsibility for final content. All authors read and approved the final manuscript.

## Declaration of Competing Interest

The authors declare that they have no known competing financial interests or personal relationships that could have appeared to influence the work reported in this paper.

## Data availability

Data will be made available on request.

## References

[1] Z.M. Younossi, P. Golabi, J.M. Paik, A. Henry, C. Van Dongen, L. Henry, The Global Epidemiology of Nonalcoholic Fatty Liver Disease (NAFLD) and Nonalcoholic Steatohepatitis (NASH): A Systematic Review. 77 (4) (2023) 1335–1347.
[2] F.-B. Lu, K.I. Zheng, R.S. Rios, G. Targher, C.D. Byrne, M.-H. Zheng, Global Epidemiology of Lean Non-Alcoholic Fatty Liver Disease: A Systematic Review and Meta-Analysis. 35 (12) (2020) 2041–2050.
[3] R. Guerrero, G.L. Vega, S.M. Grundy, J.D. Browning, Ethnic differences in hepatic steatosis: an insulin resistance paradox? Hepatology 49 (3) (2009) 791–801.
[4] K. Pafili, S. Kahl, L. Mastrototaro, K. Strassburger, D. Pesta, C. Herder, J. Pützer, B. Dewidar, M. Hendlinger, C. Granata, N. Saatmann, A. Yavas, S. Gancheva, G. Heilmann, I. Esposito, M. Schlensak, M. Roden, Mitochondrial respiration is decreased in visceral but not subcutaneous adipose tissue in obese individuals with fatty liver disease, J. Hepatol. 77 (6) (2022) 1504–1514.
[5] M. Meroni, M. Longo, G. Tria, P. Dongiovanni, Genetics Is of the Essence to Face NAFLD, Genetics Is of the Essence to Face NAFLD. 9 (10) (2021) 1359.
[6] P. Dongiovanni, M. Meroni, M. Longo, S. Fargion, A. Fracanzani, miRNA Signature in NAFLD: A Turning Point for a Non-Invasive Diagnosis. 19 (12) (2018) 3966.
[7] G. Targher, C.D. Byrne, Obesity: metabolically healthy obesity and NAFLD, Nat Rev Gastroenterol Hepatol. 13 (8) (2016) 442–444.
[8] P. Głuszyńska, D. Lemancewicz, J.B. Dzięcioł, H. Razak Hady, Non-alcoholic fatty liver disease (NAFLD) and bariatric/metabolic surgery as its treatment option: a review, J. Clin. Med. 10 (24) (2021) 5721.
[9] V. Nobili, G. Carpino, F. De Peppo, R. Caccamo, A. Mosca, I. Romito, D. Overi, A. Franchitto, P. Onori, A. Alisi, E. Gaudio, Laparoscopic sleeve gastrectomy improves nonalcoholic fatty liver disease-related liver damage in adolescents by reshaping cellular interactions and hepatic adipocytokine production, J. Pediatr. 194 (2018) 100–108.e3.
[10] N. Cabré, F. Luciano-Mateo, S. Fernández-Arroyo, G. Baiges-Gayà, A. Hernández-Aguilera, M. Fibla, R. Fernández-Julià, M. París, F. Sabench, D.D. Castillo, J. A. Menéndez, J. Camps, J. Joven, Laparoscopic sleeve gastrectomy reverses non-

alcoholic fatty liver disease modulating oxidative stress and inflammation, Metab. Clin. Exp. 99 (2019) 81–89.
[11] A.A. Salman, A.A.E.A. Sultan, A. Abdallah, A. Abdelsalam, H.M.S. Mikhail, M. Tourky, M.G. Omar, A. Youssef, R.A. Ahmed, H. Elkassar, S.M. Seif El Nasr, H.-D. Shaaban, M. Atallah, G.M.K. GabAllah, M.A. Salman, Effect of Weight Loss Induced by Laparoscopic Sleeve Gastrectomy on Liver Histology and Serum Adipokine Levels. 35 (10) (2020) 1769–1773.
[12] A. Drolz, S. Wolter, M.H. Wehmeyer, F. Piecha, T. Horvatits, J. Schulze zur Wiesch, A.W. Lohse, O. Mann, J. Kluwe, Performance of non-invasive fibrosis scores in non-alcoholic fatty liver disease with and without morbid obesity, Int. J. Obes. (Lond) 45 (10) (2021) 2197–2204.
[13] S.A. Alqahtani, P. Golabi, J.M. Paik, B. Lam, A.H. Moazez, H.A. Elariny, Z. Goodman, Z.M. Younossi, Performance of Noninvasive Liver Fibrosis Tests in Morbidly Obese Patients with Nonalcoholic Fatty Liver Disease. 31 (5) (2021) 2002–2010.
[14] S. Qadri, N. Ahlholm, I. Lønsmann, P. Pellegrini, A. Poikola, P.K. Luukkonen, K. Porthan, A. Juuti, H. Sammalkorpi, A.K. Penttilä, R. D'Ambrosio, G. Soardo, D. J. Leeming, M. Karsdal, J. Arola, S. Kechagias, S. Pelusi, M. Ekstedt, L. Valenti, H. Hagström, H. Yki-Järvinen, Obesity Modifies the Performance of Fibrosis Biomarkers in Nonalcoholic Fatty Liver Disease. 107 (5) (2022) e2008–e2020.
[15] E. Lee, H. Korf, A. Vidal-Puig, An adipocentric perspective on the development and progression of non-alcoholic fatty liver disease, J Hepatol. 78 (5) (2023) 1048–1062.
[16] G.A. Baselli, P. Dongiovanni, R. Rametta, M. Meroni, S. Pelusi, M. Maggioni, S. Badiali, P. Pingitore, S. Maurotti, T. Montalcini, A.E. Taliento, D. Prati, G. Rossi, A.L. Fracanzani, R.M. Mancina, S. Romeo, L. Valenti, Liver transcriptomics highlights interleukin-32 as novel NAFLD-related cytokine and candidate biomarker, Gut 69 (10) (2020) 1855–1866.
[17] M. Meroni, M. Longo, E. Paolini, R. Lombardi, R. Piciotti, P. Francione, S. Badiali, M. Maggioni, A.L. Fracanzani, P. Dongiovanni, MAFLD definition underestimates the risk to develop HCC in genetically predisposed patients, J. Intern. Med. 291 (3) (2022) 374–376.
[18] N. Panera, M. Meroni, M. Longo, A. Crudele, L. Valenti, E. Bellacchio, L. Miele, V. D'Oria, E. Paolini, M. Maggioni, A.L. Fracanzani, A. Alisi, P. Dongiovanni, The KLB rs17618244 gene variant is associated with fibrosing MAFLD by promoting hepatic stellate cell activation, EBioMedicine 65 (2021), 103249.
[19] R.E. Kavey, S.R. Daniels, R.M. Lauer, D.L. Atkins, L.L. Hayman, K. Taubert, American Heart Association guidelines for primary prevention of atherosclerotic cardiovascular disease beginning in childhood, Circulation 107 (11) (2003) 1562–1566.
[20] D.E. Kleiner, E.M. Brunt, M. Van Natta, C. Behling, M.J. Contos, O.W. Cummings, L. D. Ferrell, Y.-C. Liu, M.S. Torbenson, A. Unalp-Arida, M. Yeh, A.J. McCullough, A. J. Sanyal, Design and validation of a histological scoring system for nonalcoholic fatty liver disease, Hepatology 41 (6) (2005) 1313–1321.
[21] M. Longo, M. Meroni, E. Paolini, V. Erconi, F. Carli, F. Fortunato, et al., TM6SF2/PNPLA3/MBOAT7 loss-of-function genetic variants impact on NAFLD development and progression both in patients and in in vitro models, Cell Mol. Gastroenterol. Hepatol. (2021).
[22] M. Meroni, P. Dongiovanni, PNPLA3 rs738409 genetic variant inversely correlates with platelet count, thereby affecting the performance of noninvasive scores of hepatic fibrosis, Int J Mol Sci. 24 (20) (2023) 15046.
[23] J.T. Leek, svaseq: removing batch effects and other unwanted noise from sequencing data, Nucleic Acids Res. 42 (21) (2014) e161.
[24] M.I. Love, W. Huber, S. Anders, Moderated estimation of fold change and dispersion for RNA-seq data with DESeq2, Genome Biol. 15 (12) (2014) 550.
[25] W. Luo, M.S. Friedman, K. Shedden, K.D. Hankenson, P.J. Woolf, GAGE: generally applicable gene set enrichment for pathway analysis, BMC Bioinf. 10 (2009) 161.
[26] M. Kanehisa, S. Goto, KEGG: kyoto encyclopedia of genes and genomes, Nucleic Acids Res. 28 (1) (2000) 27–30.
[27] A. Liberzon, C. Birger, H. Thorvaldsdóttir, M. Ghandi, J.P. Mesirov, P. Tamayo, The molecular signatures database (MSigDB) hallmark gene set collection, Cell Syst. 1 (6) (2015) 417–425.
[28] M. Ashburner, C.A. Ball, J.A. Blake, D. Botstein, H. Butler, J.M. Cherry, A.P. Davis, K. Dolinski, S.S. Dwight, J.T. Eppig, M.A. Harris, D.P. Hill, L. Issel-Tarver, A. Kasarskis, S. Lewis, J.C. Matese, J.E. Richardson, M. Ringwald, G.M. Rubin, G. Sherlock, Gene ontology: tool for the unification of biology, The Gene Ontology Consortium. Nat Genet. 25 (1) (2000) 25–29.
[29] Gu Z, Hübschmann D. simplifyEnrichment: an R/Bioconductor package for Clustering and Visualizing Functional Enrichment Results. bioRxiv. 2021:2020.10.27.312116.
[30] E. Edelman, A. Porrello, J. Guinney, B. Balakumaran, A. Bild, P.G. Febbo, et al. Analysis of sample set enrichment scores: assaying the enrichment of sets of genes for individual samples in genome-wide expression profiles. Bioinformatics. 2006; 22(14):e108-16.
[31] S. Hänzelmann, R. Castelo, J. Guinney, GSVA: gene set variation analysis for microarray and RNA-seq data, BMC Bioinf. 14 (2013) 7.
[32] M. Bombaci, R.L. Rossi, Computation and Selection of optimal biomarker combinations by integrative ROC analysis using combiROC, Methods Mol Biol. 1959 (2019) 247–259.
[33] D. Türei, T. Korcsmáros, J. Saez-Rodriguez, OmniPath: guidelines and gateway for literature-curated signaling pathway resources, Nat Methods. 13 (12) (2016) 966–967.
[34] P.J. Thul, C. Lindskog, The human protein atlas: a spatial map of the human proteome, Protein Sci. 27 (1) (2018) 233–244.
[35] M. Bersanelli, E. Mosca, D. Remondini, G. Castellani, L. Milanesi, Network diffusion-based analysis of high-throughput data for the detection of differentially enriched modules, Sci Rep. 6 (2016) 34841.
[36] N. Di Nanni, M. Bersanelli, L. Milanesi, E. Mosca, Network diffusion promotes the integrative analysis of multiple omics, Front Genet. 11 (2020) 106.
[37] D. Szklarczyk, A. Franceschini, S. Wyder, K. Forslund, D. Heller, J. Huerta-Cepas, M. Simonovic, A. Roth, A. Santos, K.P. Tsafou, M. Kuhn, P. Bork, L.J. Jensen, C. von Mering, STRING v10: protein-protein interaction networks, integrated over the tree of life, Nucleic Acids Res. 43 (D1) (2015) D447–D452.
[38] N. Di Nanni, M. Gnocchi, M. Moscatelli, L. Milanesi, E. Mosca, I. Birol, Gene relevance based on multiple evidences in complex networks, Bioinformatics 36 (3) (2020) 865–871.
[39] M. Lopez-Yus, S. Lorente-Cebrian, R. del Moral-Bergos, C. Hörndler, M.P. Garcia-Sobreviela, C. Casamayor, A. Sanz-Paris, V. Bernal-Monterde, J.M. Arbones-Mainar, Identification of novel targets in adipose tissue involved in non-alcoholic fatty liver disease progression, Faseb J. 36 (8) (2022) e22429.
[40] R. Diaz Marin, S. Crespo-Garcia, A.M. Wilson, P. Sapieha, RELi protocol: optimization for protein extraction from white, brown and beige adipose tissues, MethodsX. 6 (2019) 918–928.
[41] R.P. Wildman, P. Muntner, K. Reynolds, A.P. McGinn, S. Rajpathak, J. Wylie-Rosett, et al., The obese without cardiometabolic risk factor clustering and the normal weight with cardiometabolic risk factor clustering: prevalence and correlates of 2 phenotypes among the US population (NHANES 1999–2004), Arch Intern Med. 168 (15) (2008) 1617–1624.
[42] J. Cao, L. Cheng, Y. Shi, Catalytic properties of MGAT3, a putative triacylgycerol synthase, J. Lipid Res. 48 (3) (2007) 583–591.
[43] L.E. Dichtel, K.E. Corey, J. Misdraji, M.A. Bredella, M. Schorr, S.A. Osganian, B. J. Young, J.C. Sung, K.K. Miller, The association between IGF-1 levels and the histologic severity of nonalcoholic fatty liver disease, Clin Transl Gastroenterol. 8 (1) (2017) e217.
[44] V. Marques, M.B. Afonso, N. Bierig, F. Duarte-Ramos, Á. Santos-Laso, R. Jimenez-Agüero, E. Eizaguirre, L. Bujanda, M.J. Pareja, R. Luís, A. Costa, M.V. Machado, C. Alonso, E. Arretxe, J.M. Alustiza, M. Krawczyk, F. Lammert, D.G. Tiniakos, B. Flehmig, H. Cortez-Pinto, J.M. Banales, R.E. Castro, A. Normann, C.M. P. Rodrigues, Adiponectin, leptin, and IGF-1 are useful diagnostic and stratification biomarkers of NAFLD, Front Med (lausanne). 8 (2021), 683250.
[45] I. Brandão, M.J. Martins, R. Monteiro, Metabolically healthy obesity-heterogeneity in definitions and unconventional factors, Metabolites 10 (2) (2020) 48.
[46] J. Nilsson, S. Jovinge, A. Niemann, R. Reneland, H. Lithell, Relation between plasma tumor necrosis factor-alpha and insulin sensitivity in elderly men with non-insulin-dependent diabetes mellitus, Arterioscler. Thromb. Vasc. Biol. 18 (8) (1998) 1199–1202.
[47] G. Huang, H. Li, H. Zhang, Abnormal expression of mitochondrial ribosomal proteins and their encoding genes with cell apoptosis and diseases, Int. J. Mol. Sci. 21 (22) (2020) 8879.
[48] M. Longo, M. Meroni, E. Paolini, C. Macchi, P. Dongiovanni, Mitochondrial dynamics and nonalcoholic fatty liver disease (NAFLD): new perspectives for a fairy-tale ending? Metabolism 117 (2021), 154708.
[49] S.A. Harrison, M.R. Bashir, C.D. Guy, R. Zhou, C.A. Moylan, J.P. Frias, N. Alkhouri, M.B. Bansal, S. Baum, B.A. Neuschwander-Tetri, R. Taub, S.E. Moussa, Resmetirom (MGL-3196) for the treatment of non-alcoholic steatohepatitis: a multicentre, randomised, double-blind, placebo-controlled, phase 2 trial, Lancet 394 (10213) (2019) 2012–2024.
[50] S. Heinonen, J. Buzkova, M. Muniandy, R. Kaksonen, M. Ollikainen, K. Ismail, A. Hakkarainen, J. Lundbom, N. Lundbom, K. Vuolteenaho, E. Moilanen, J. Kaprio, A. Rissanen, A. Suomalainen, K.H. Pietiläinen, Impaired mitochondrial biogenesis in adipose tissue in acquired obesity, Diabetes 64 (9) (2015) 3135–3145.
[51] H.R. Chang, H.J. Kim, X. Xu, A.W. Ferrante Jr., Macrophage and adipocyte IGF1 maintain adipose tissue homeostasis during metabolic stresses, Obesity (silver Spring, Md). 24 (1) (2016) 172–183.
[52] M.S. Lewitt. The role of the growth hormone/insulin-like growth factor system in visceral adiposity. Biochemistry insights. 2017;10:1178626417703995.
[53] S. Subudhi, H.K. Drescher, L.E. Dichtel, L.M. Bartsch, R.T. Chung, M.M. Hutter, D. W. Gee, O.R. Meireles, E.R. Witkowski, L. Gelrud, R. Masia, S.A. Osganian, J. L. Gustafson, S. Rwema, M.A. Bredella, S.N. Bhatia, A. Warren, K.K. Miller, G. M. Lauer, K.E. Corey, Distinct hepatic gene-expression patterns of NAFLD in patients with obesity, Hepatol Commun. 6 (1) (2022) 77–89.
[54] R.J. Schleifer, S. Li, W. Nechtman, E. Miller, S. Bai, A. Sharma, J.-X. She, KLHL5 knockdown increases cellular sensitivity to anticancer drugs, Oncotarget 9 (100) (2018) 37429–37438.
[55] M. Kouvari, N. M. D'Cunha, T. Tsiampalis, M. Zec, D. Sergi, N. Travica, W. Marx, A. J. McKune, D.B. Panagiotakos, N. Naumovski, Metabolically healthy overweight and obesity, transition to metabolically unhealthy status and cognitive function: results from the framingham offspring study, Nutrients 15 (5) (2023) 1289.